Electronic Supplementary Material (ESI) for Journal of Materials Chemistry C.
This journal is © The Royal Society of Chemistry 2023

Transport properties of GNR-C_{60} single-molecule devices

Xiaohui Liu, Yangyang Hu*, Danting Li, Guiling Zhang*

School of Materials Science and Engineering, Harbin University of Science and Technology, Harbin 150080, China.*e-mail: guiling-002@163.com and 937972827@qq.com

Impact of Linkage Position and Passivated Edge on the MPSH states, LDOS and Effective Potential Distributions

Taken the H-passivated devices (D-H/AA', D-H/BB', D-H/AB', and D-H/ABA'B') as examples, we compare the differences of MPSH states, LDOS and effective potential distributions in devices with different linkage positions but the same passivated edge, as shown in Fig 1-8. For the MPSH state, electron hoping along the molecule is allowed and the channel is open if the HOMO and LUMO are distributed in different sides respectively. From Fig 1-4, their HOMO and LUMO either locate on the same side or the C_{60} and one side at 0.0 V, the tunneling channel is closed. When the applied voltage increases to 0.2 V, the HOMO and LUMO trend to cross, resulting the first NDR peaks. Notably, the majority the HOMO locates on C_{60} and the minority on the right side, while the LUMO evenly distribute on C_{60} and the left side in D-H/BB'. That is, the crossing of the HOMO and LUMO is relatively weak in D-H/BB', related to its smallest conductivity at 0.2 V compared with the other three H-passivated devices. With the applied voltage increasing, the HOMO and LUMO localized on certain region, the crossing of the HOMO and LUMO disappear, leading the tunneling channel closed again. Until the applied voltage arriving to 1.2 V, obvious crossing of the HOMO and LUMO can be observed, causing the second, also the biggest NDR peaks in the four devices. Such crossing is particularly evident in the case of D-H/ABA'B', in line with its largest conductivity. The distributions of LDOS and voltage drop of the four devices are shown in Fig. 5-8. All the LDOS at 0.2 and 1.2 V applied voltage are more evident and even well-spread than those at other applied voltage. Significantly, the C_{60} participate in the conductivity at high applied

voltage in D-H/ABA'B', which is nearly absent in the case of D-H/AA', D-H/BB', and D-H/AB', demonstrating the superiority of ABA'B' linkage positions in the transport properties. At the same time, smaller voltage drops (more green in Fig. 5-8) can be detected at 0.2 and 1.2 V. Among them, the voltage drop under 0.2 V in D-H/BB' is larger than those of the other three, while that under 1.2 V is larger than those of the other three in D-H/AB', in good accordance with transmission spectra and NDR.

On the other hand, taken the three devices D-H/ABA'B', D-O/ABA'B' and D-S/ABA'B' as examples, we compare the differences of MPSH states, LDOS and effective potential distributions in devices with the same linkage position but different passivated edges, as shown in Fig. 4, 9-10, and 8, 11-12. From Fig. 4, 9-10, impacted by the large electronegativity of O and S atoms, most the FMOs localize on the passivated edges. This is disadvantage for the crossing of the HOMO and LUMO, so the conductivity is significantly reduced. Current is small in D-O/ABA'B', negligible NDR behavior can be detected. Due to the weaker electronegativity of S compared with O, crossing of the HOMO and LUMO exists in D-S/ABA'B' at 0.2 V. The total conductivity of D-S/ABA'B' is smaller than D-H/ABA'B', but higher than D-O/ABA'B'. It is difficult to notice evident and even well-spread LDOS in D-O/ABA'B' and D-S/ABA'B', the voltage drops of them also much smaller than that of D-H/ABA'B', in good accordance with our previous discussions.

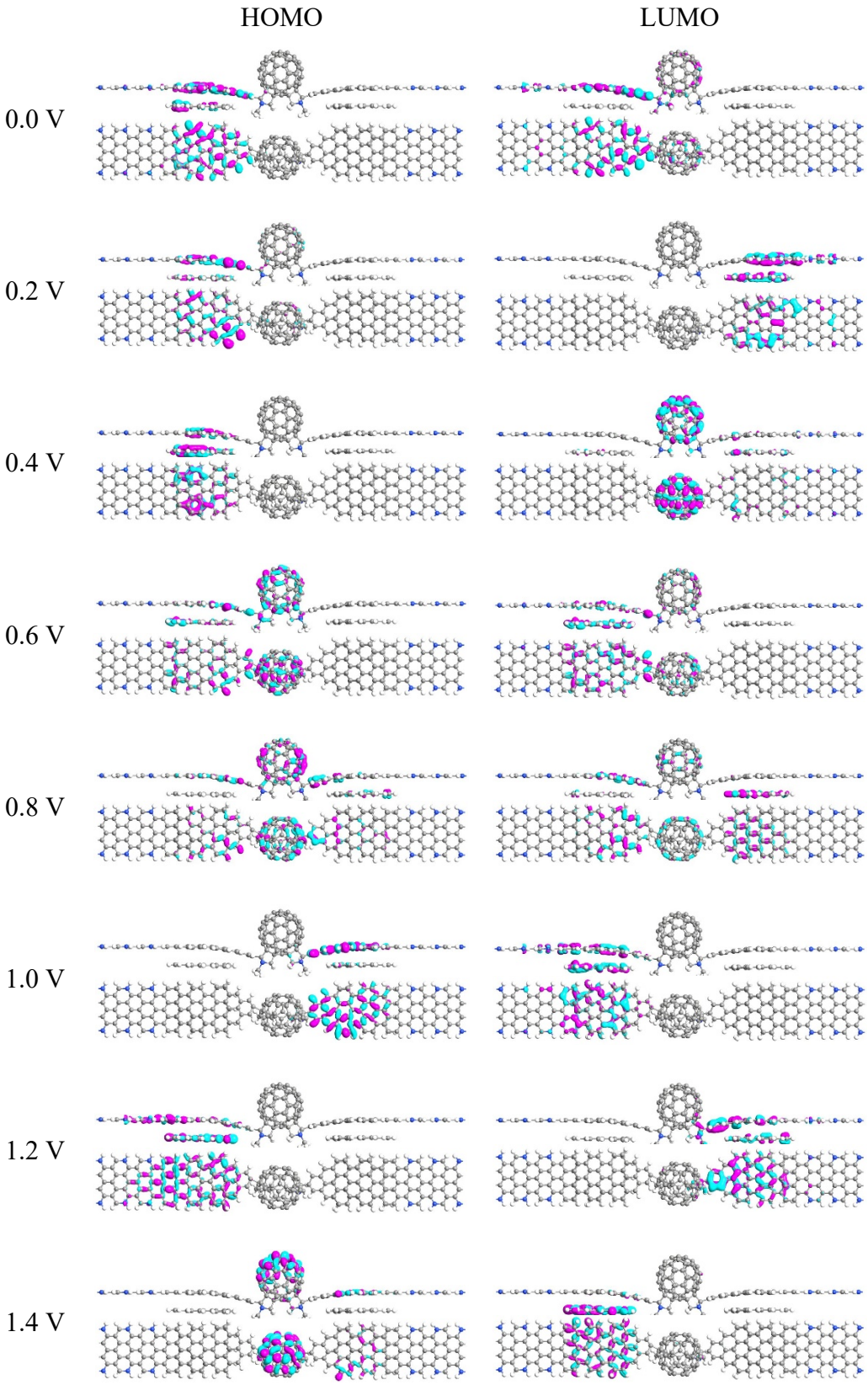

Figure 1 The calculated MPSH states of FMOs for the D-H/AA′ two-probe device at different bias voltages.

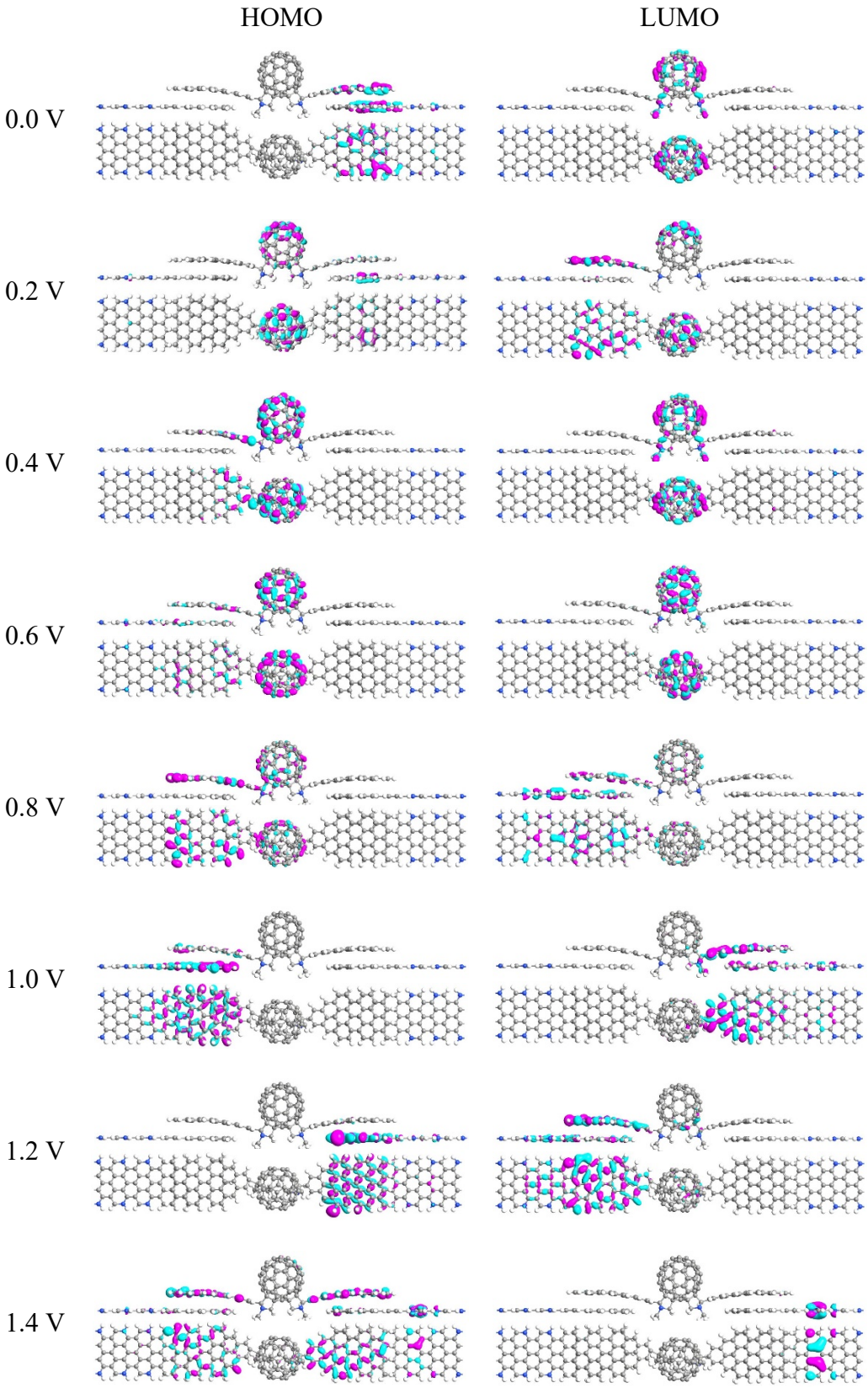

Figure 2 The calculated MPSH states of FMOs for the D-H/BB′ two-probe device at different bias voltages.

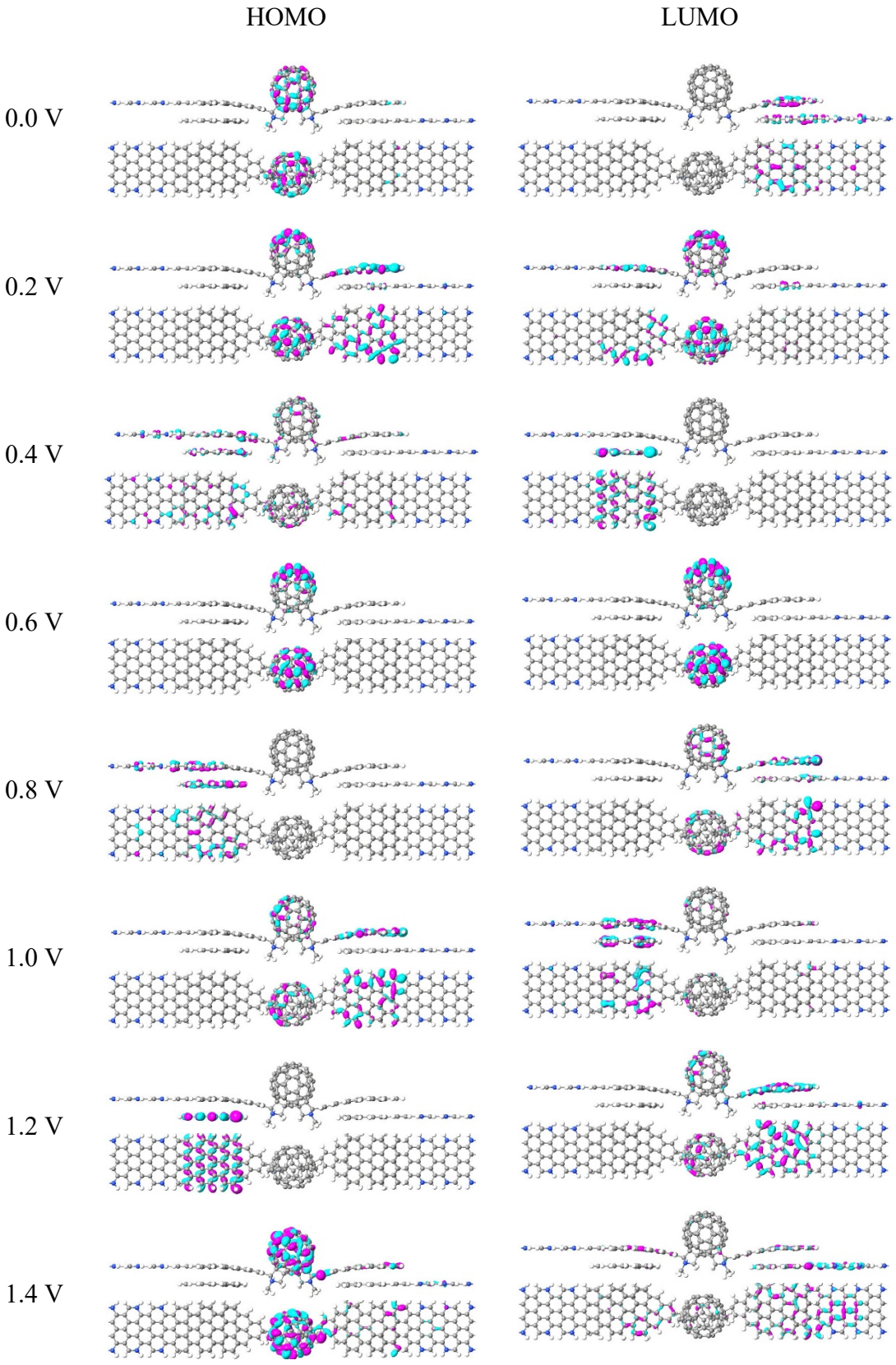

Figure 3 The calculated MPSH states of FMOs for the D-H/AB′ two-probe device at different bias voltages.

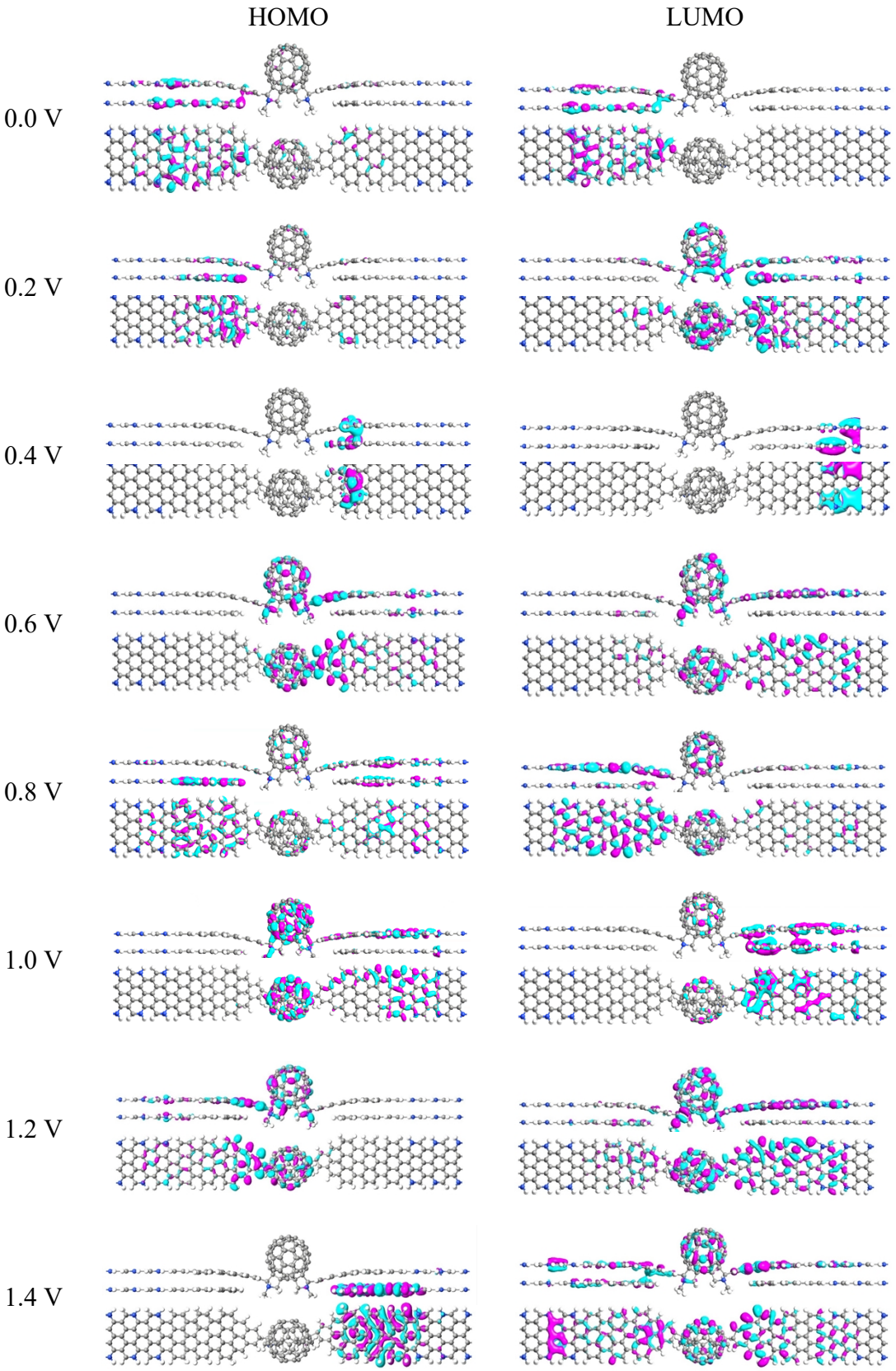

Figure 4 The calculated MPSH states of FMOs for the D-H/ABA′B′ two-probe device at different bias.

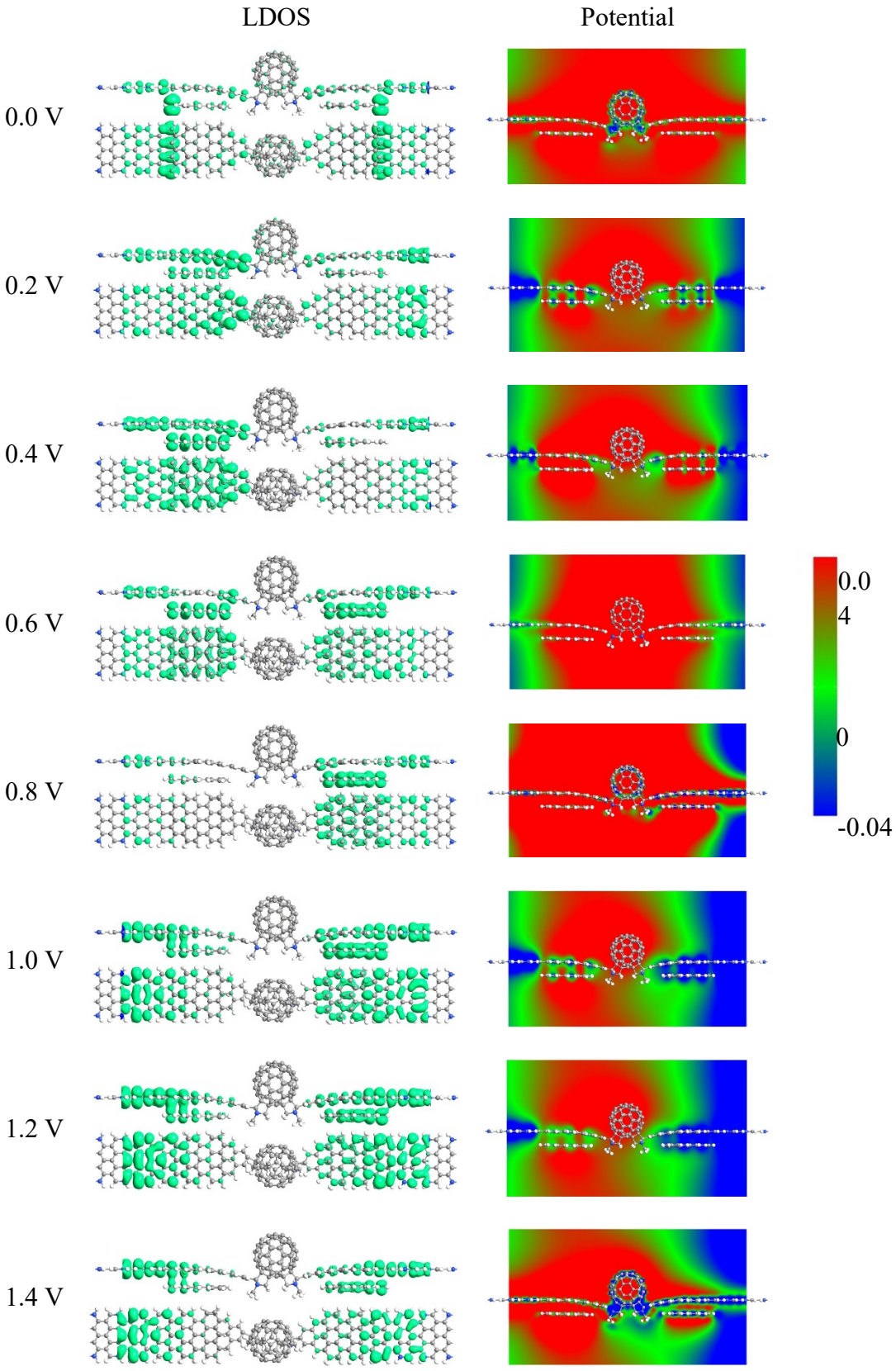

Figure 5 LDOS and effective potential distributions of D-H/AA′ two-probe device at different bias voltages.

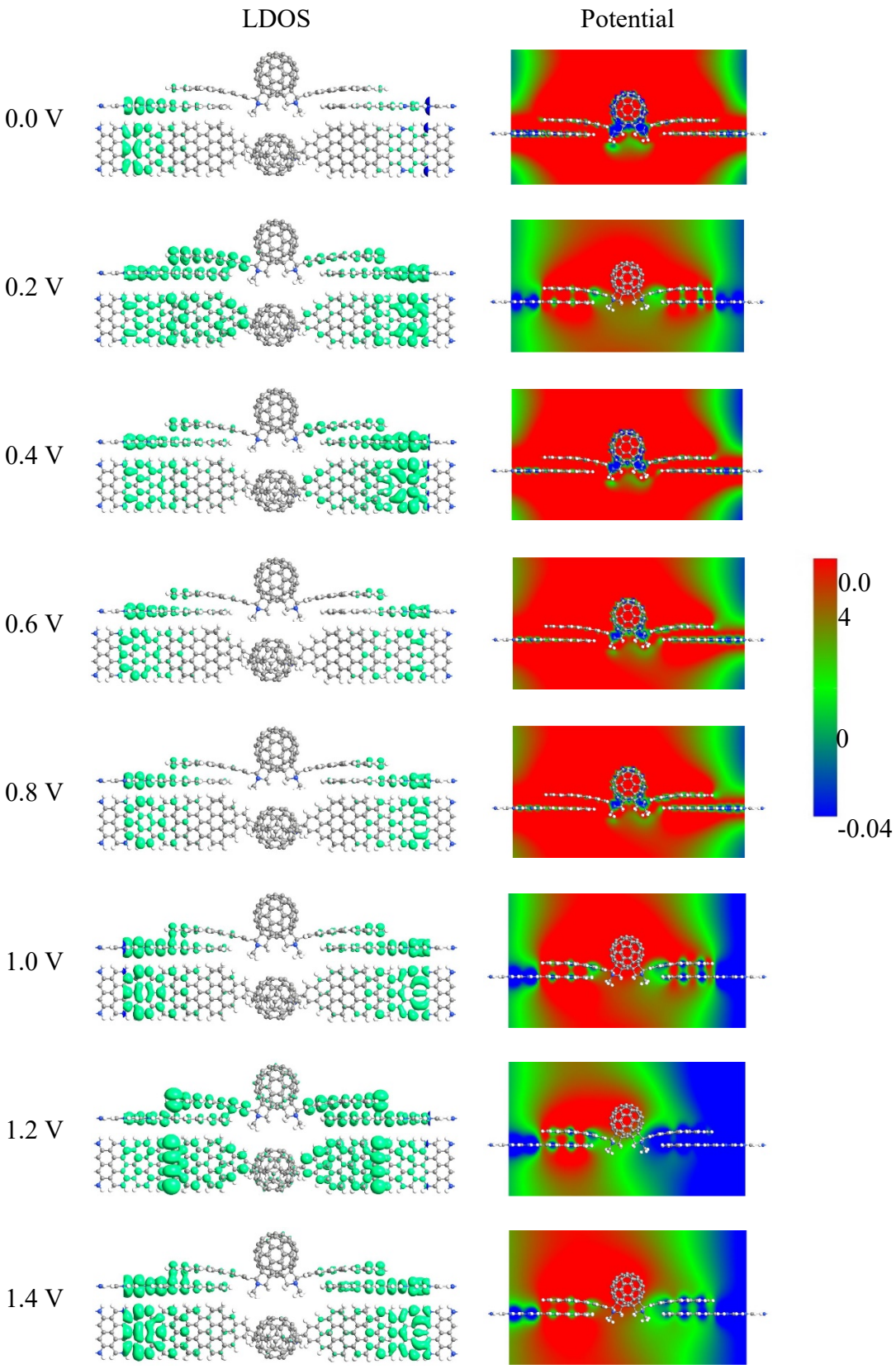

Figure 6 LDOS and effective potential distributions of D-H/BB′ two-probe device at different bias voltages.

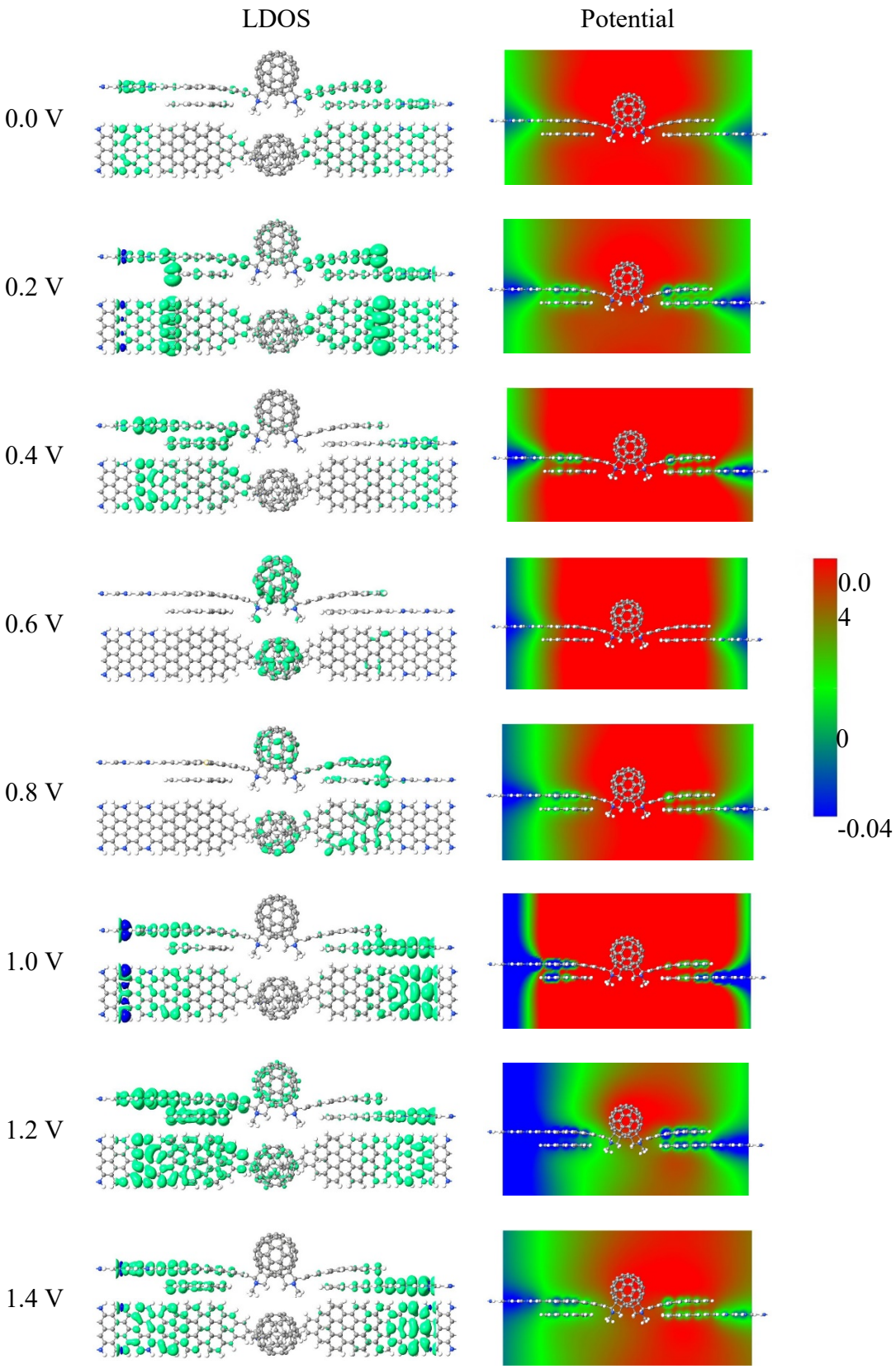

Figure 7 LDOS and effective potential distributions of D-H/AB′ two-probe device at different bias voltages.

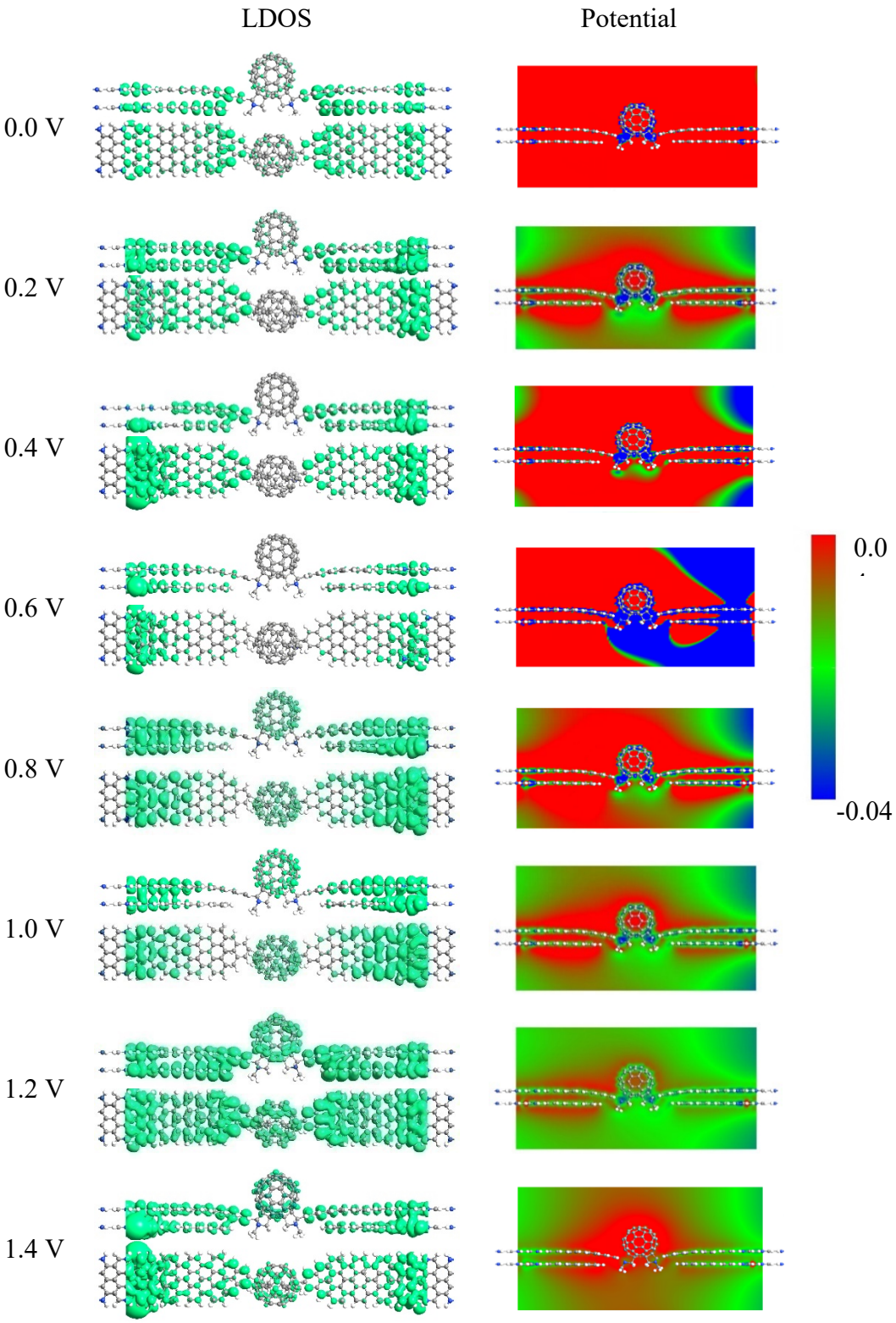

Figure 8 LDOS and effective potential distributions of D-H/ABA′B′ two-probe device at different bias voltages.

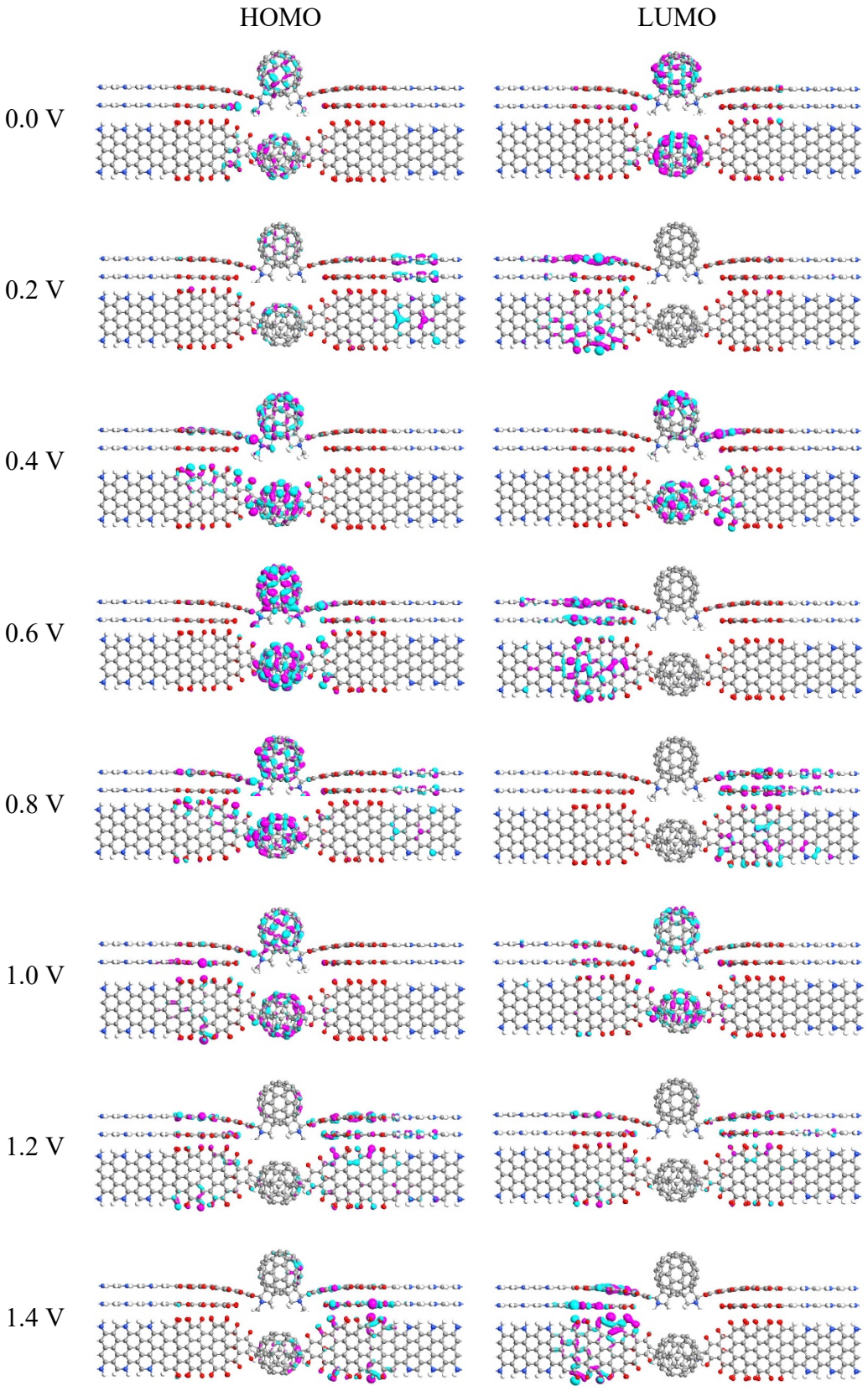

Figure 9 The calculated MPSH states of FMOs for the D-O/ABA'B' two-probe device at different bias voltages.

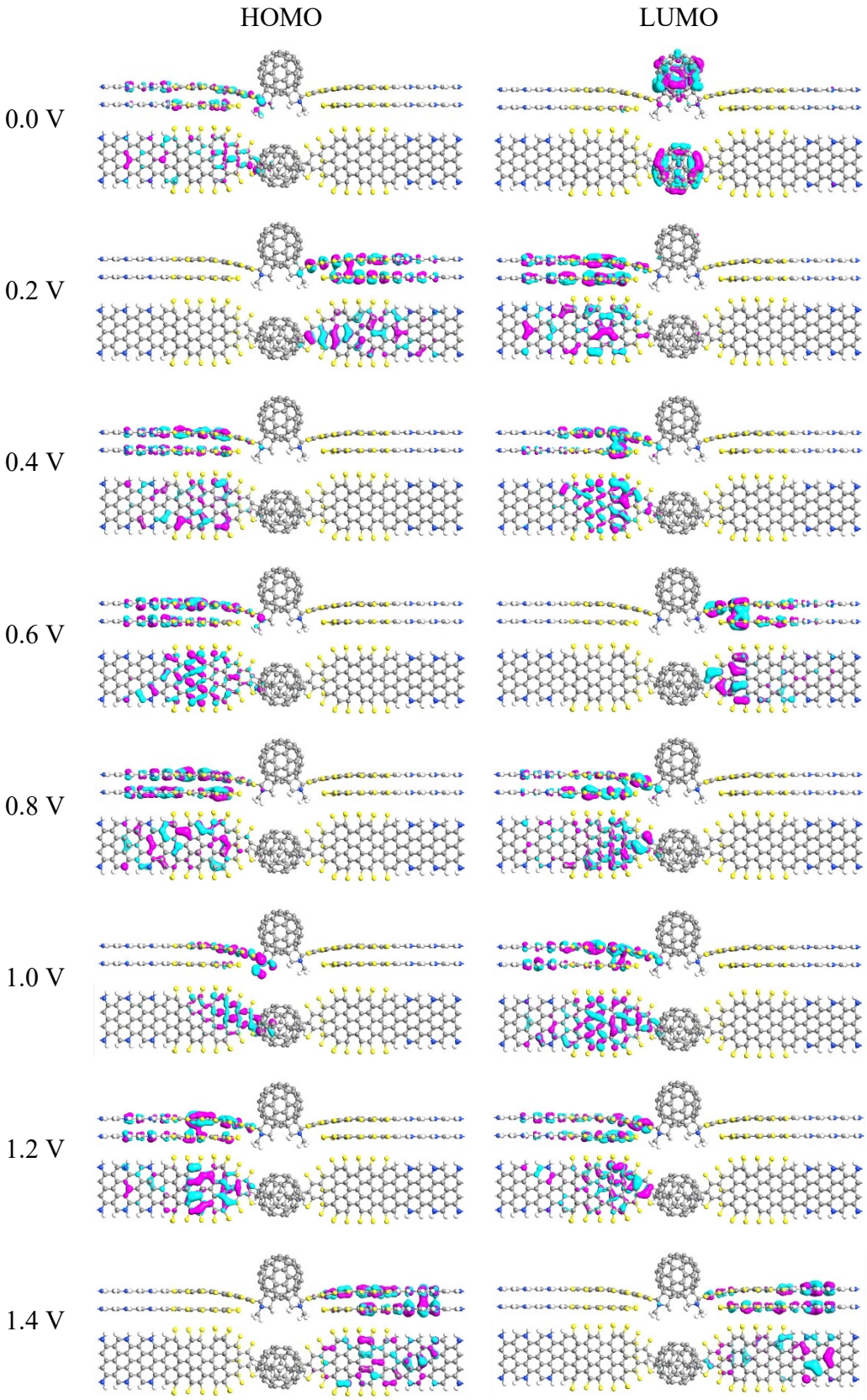

Figure 10 The calculated MPSH states of FMOs for the D-S/ABA'B' two-probe device at different bias voltages.

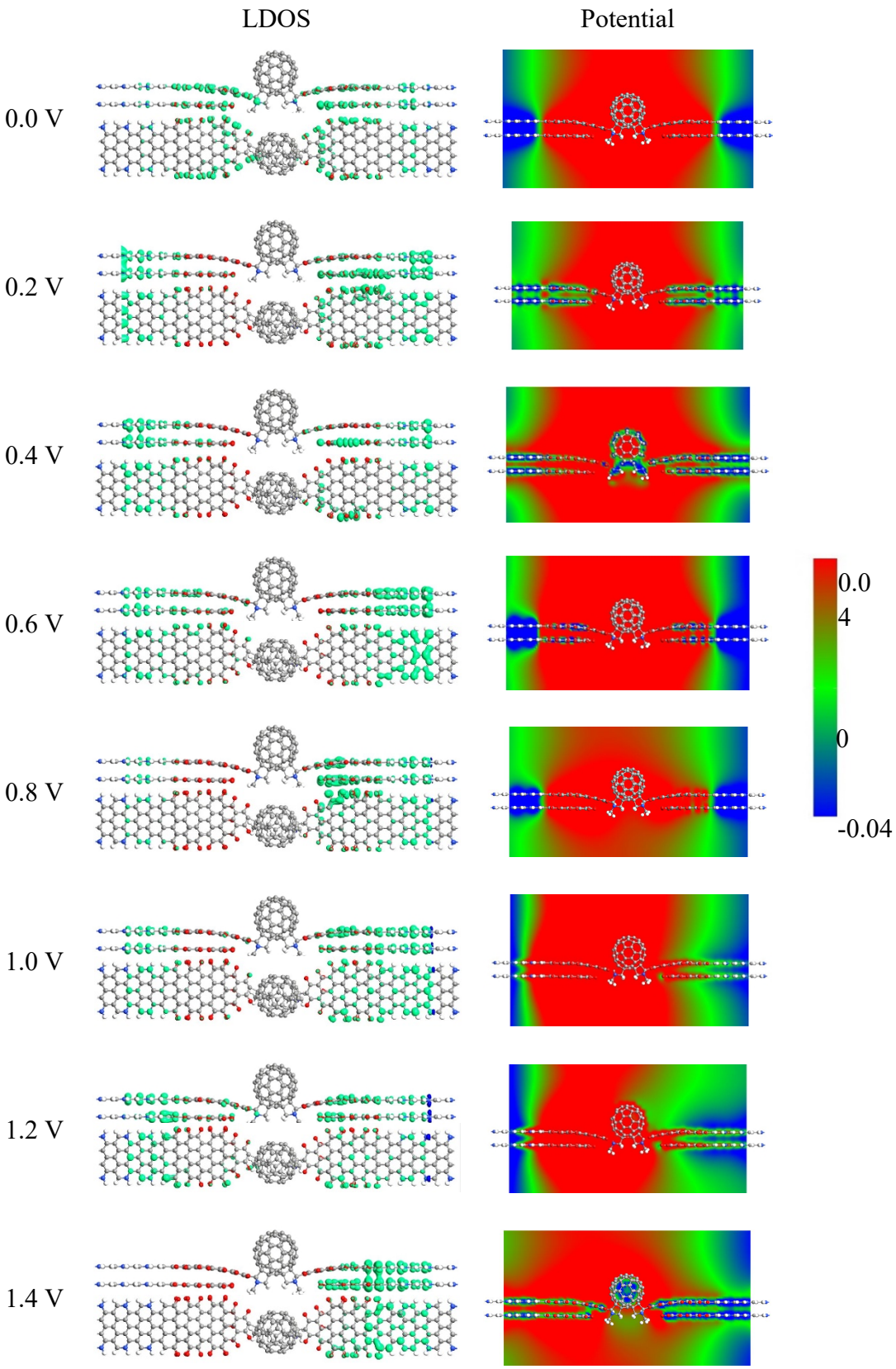

Figure 11 LDOS and effective potential distributions of D-O/ABA'B' two-probe device at different bias voltages.

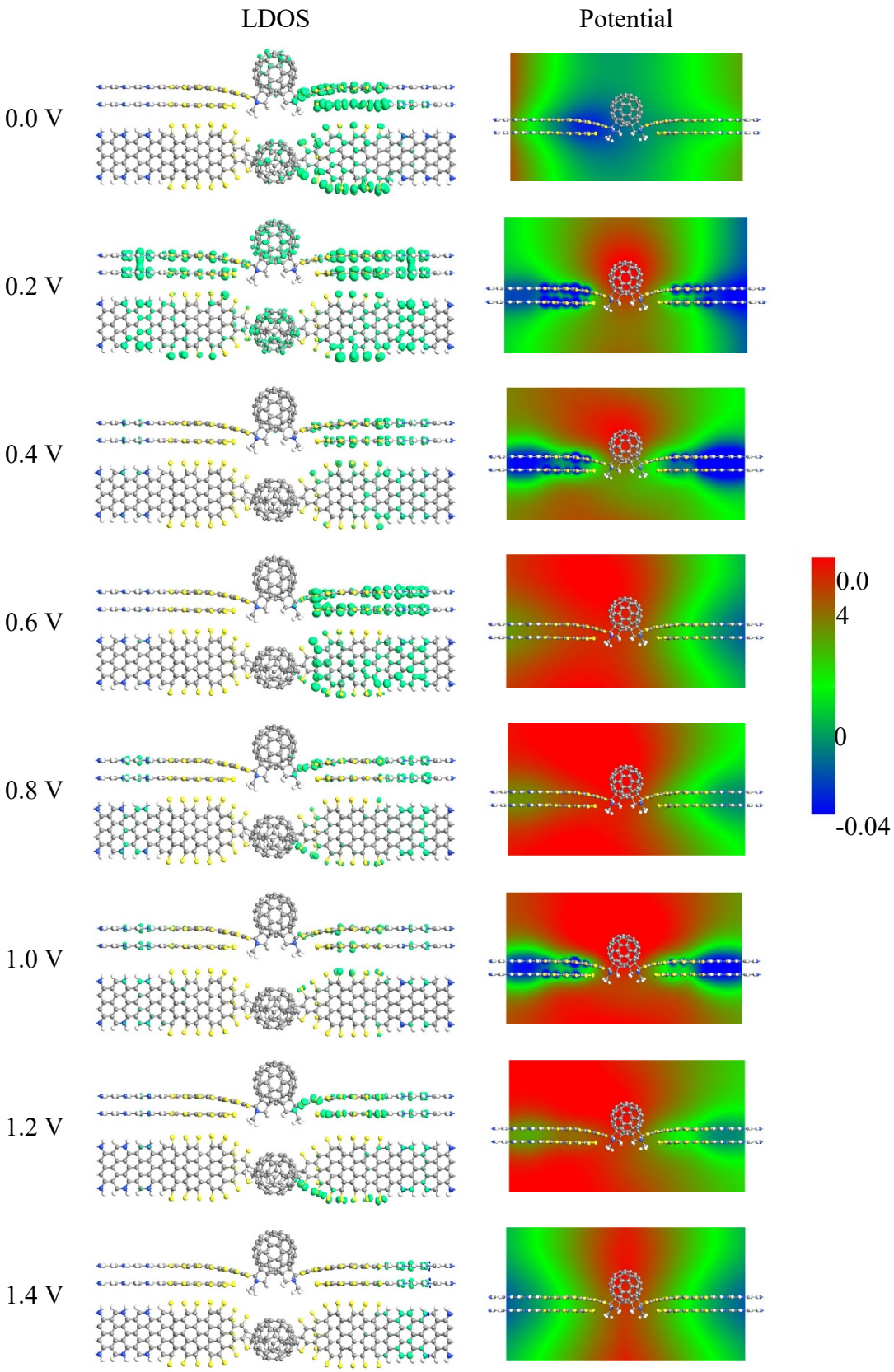

Figure 12 LDOS and effective potential distributions of D-S/ABA'B' two-probe device at different bias voltages.